Int. J. Adv. Appl. Math. and Mech. 7(4) (2020) 1 – 13 (ISSN: 2347-2529)

Journal homepage: www.ijaamm.com

IJAAMM

International Journal of Advances in Applied Mathematics and Mechanics

Hydromagnetic couette flow between two vertical semi infinite permeable plates

Research Article

Otieno Collins Owuor[a,*], M. N Kinyanjui [b], P. R Kiogora[b]

[a] *Jomo Kenyatta University of Agriculture and Technology, Juja, 62000-00200, Nairobi, Kenya*

[b] *Department of Pure and Applied Mathematics,Jomo Kenyatta University of Agriculture and Technology, Juja, 62000-00200, Nairobi, Kenya*

Received 26 January 2020; accepted (in revised version) 19 March 2020

Abstract: In this paper, the hydromagnetic couette flow between the two vertical semi-infinite permeable plates with uniform injection/suction in the presence of a constant magnetic field applied normal to the fluid flow while considering joule heating is considered. The fluid flow is unsteady, viscous, incompressible and electrically conducting. The final non-linear partial differential equations governing this flow problem is solved numerically using finite difference method and the results are analyzed using MATLAB and represented graphically. The effects of various non-dimensional parameters such as Reynolds Number, Eckert Number and other non-dimensional parameters on velocity and temperature profiles are discussed into details. The effects of varying various parameters led to either increase, decrease or no effect on flow variables.

The MHD Couette flow between permeable plates that has been studied in this research has many applications in areas such as purification of crude oil, petroleum industry, aerodynamic heating, electrostatic precipitation, polymer technology, accelerators, MHD pumps, power generators and many others.

MSC: 80Axx • 92Bxx

Keywords: Couette • permeable • Unsteadiness

Magneto hydrodynamics has been of interest in the recent past due to its wide spread application in petroleum industry, aerodynamic heating, electrostatic precipitation, polymer technology, accelerators, purification of crude oil, MHD pumps and power generators. The word magneto hydrodynamic (MHD) is derived from; Magneto-meaning magnetic field, hydro-meaning liquid and dynamics which means movement. Magneto hydrodynamics as a word has been used by several researchers including [1]. Couette flow is a laminar flow of a viscous fluid in the space between two parallel plates where one plate moves relative to the other. The flow is driven by virtue of the viscous drag force which acts on the fluid but may be additionally be motivated by an applied pressure gradient in the flow direction. This type of flow is named in honor of Maurice Marie Alfred Couette, a professor of Physics in French university of Angers in the late 19^{th} century. Porous medium is a material containing pores or voids. Porosity or void fraction is the measure of the empty spaces(void) in a material as defined by [2]. A non-porous material is one that is not permeable to fluids. Permeability is the measure of the ability of a porous material to allow fluids to pass through it. [3] investigated unsteady hydromagnetic Couette flow of a viscous, incompressible and electrically conducting fluid under the influence of a uniform transverse magnetic field when the fluid flow within the channel is induced due to impulsive

* Corresponding author.

E-mail address(es): owuorcollins@yahoo.com (Otieno Collins Owuor), mkinyanjui@fsc.jkuat.ac.ke (M.N Kinyanjui), prkiogora@fsc.jkuat.ac.ke (P.R Kiogora).

movement of one of the plates of the channel. [4] analyzed this problem in a channel between parallel porous plates where the fluid flow within the channel is induced as a result of uniform accelerated movement of one of the channel. [5] discussed effect of induced magnetic field on a flow within a porous channel when the fluid flow within the channel is induced due to uniformly accelerated motion when one of the plates starts moving with a time dependent velocity. [6] studied MHD Couette flow of a viscous, incompressible and electrically conducting fluid in the presence of a uniform transverse magnetic field when the fluid flow within the channel is induced due to time dependent movement of one of the plate and magnetic field is fixed relative to the moving plate. [7] studied the heat transfer in porous medium in the presence of transverse magnetic field. The effects of the heat source parameter and Nusselt number were analyzed and discovered that the effect of increasing porous parameter is to increase the Nusselt number. [8] investigated MHD Stokes problem for a vertical infinite plate in dissipative rotating fluid with Hall current. [9] studied natural convection in unsteady hydro magnetic Couette flow through a vertical channel in the presence of thermal radiation. The effect of different parameters like magnetic parameter, Prandtl number, radiation parameter, thermal Grashof number, accelerating parameter and time on the temperature, velocity, skin friction and Nusselt number were discussed. [11] considered unsteady MHD Couette flow with heat transfer of a viscoelastic fluid exponential decaying pressure gradient. It was found that the viscoelastic parameter had a marked effect on the velocity and temperature distributions and their steady state times for all values of the magnetic field and the suction velocity. Also [11] reported unsteady MHD Couette flow of a viscoelastic fluid with heat transfer. [12] investigated flow formation in Couette motion in magneto hydrodynamics with time varying suction and taking into account the effects of heat and mass transfer. [13] studied the problem when the fluid flow is confined to porous boundaries with suction and injection. It was concluded that the suction exerted a retarding influence on the fluid velocity whereas injection has accelerating influence on the flow while the magnetic field, time and injection reduces shear stress at lower plate. [20] studied the problem of steady hydromagnetic Couette flow of a highly viscous fluid through a porous channel in the presence of an applied uniform transverse magnetic field and thermal radiation. [15] investigated unsteady MHD convective flow past an infinite vertical porous plate in an incompressible electrically conducting fluid. The numerical results of the study showed that an increase in the Grashof number causes an increase in the velocity profiles, an increase of Hartman number causes a decrease of velocity profile. [16] investigated unsteady magneto hydrodynamic free convective Couette flow between two vertical permeable plates in the presence of thermal radiation using Galerkin's finite method. [17] investigated unsteady natural convective Couette flow of a reactive viscous fluid in a vertical channel. [18] investigated unsteady MHD Couette flow between two infinite parallel plates in an inclined magnetic field with heat transfer. The lower plate was considered stationary and porous. He found out that an increase in the magnetic number lead to a decrease in the velocity of the fluid. [22] investigated steady hydromagnetic flow between two infinite parallel vertical porous plate. The effect of different parameter such as magnetic parameter, Prandtl number, thermal Grashof number, temperature and velocity distributions were discussed. [20] investigated unsteady hydromagnetic Couette flow with magnetic field lines fixed relative to the moving upper plate with suction and injection. It was found that the magnetic field, pressure gradient, time and injection have an accelerating influence whereas suction and viscosity exerts a retarding influence on the fluid flow between parallel porous plate with injection/suction and constant pressure gradient applied in the direction of the flow. [21] investigated a turbulent incompressible fluid flow past a semi-infinite vertical rotating plate in the presence of a strong inclined constant magnetic field. It was found out that an increase in the angle of inclination leads to an increase in the primary velocity while an increase in Eckert number leads to a decrease in the primary velocity profiles. [22] analyzed steady convective MHD fluid flow in parallel semi-infinite plates with constant magnetic field. Hartmann and Prandtl numbers were found to have a great effect on velocity profiles and temperature distribution respectively whereby an increase in Hartmann number causes a decrease in velocity profiles while an increase in Prandtl number leads to a fall in temperature. [23] investigated unsteady MHD free convective Couette flow between vertical porous plates with thermal radiation. It was found that velocity and temperature field increases with increase in time and also skin friction increases with increase in time while Nusselt number decreases with increase in time. In view of the above studies, no consideration has been given on unsteady hydromagnetic Couette flow between two vertical semi-infinite permeable plates with uniform suction and injection considering joule heating.

1. Mathematical Model

The fundamentals of fluid dynamics are based on universal laws that govern fluid flows such as the equation of continuity, equation of motion, equation of energy and the electromagnetic equation. The governing equations discussed in this section includes the equation of continuity, equation of motion, equation of energy and the electromagnetic equations.

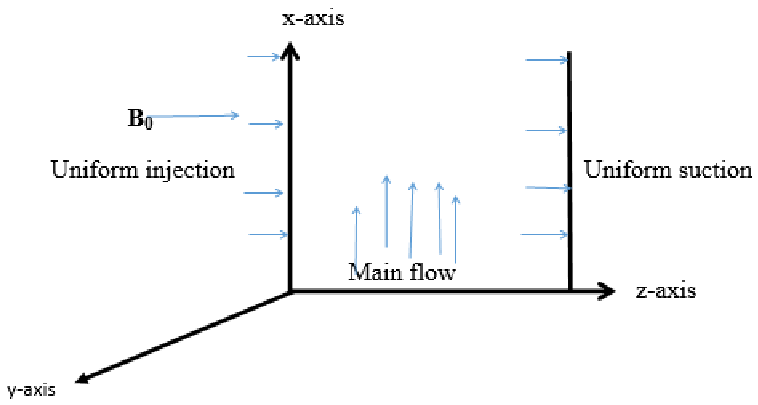

Fig. 1. Geometry of the flow

2. Governing equations

2.1. Equation of continuity

The equation of continuity is derived from the law of conservation of mass which states that under normal conditions mass can neither be created nor destroyed. It is derived by taking a mass balance on the fluid entering and leaving a volume element in the flow field. The general equation of continuity of a fluid flow is given :

$$\frac{\partial \rho}{\partial t} + \vec{\nabla}.\left(\rho \vec{q}\right) = 0 \tag{1}$$

where $\vec{q} = u\hat{i} + v\hat{j} + w\hat{k}$ is the velocity vector in the x,y and z-directions. In tensor form the equation is:

$$\frac{\partial \rho}{\partial t} + \frac{\partial}{\partial x_i}(\rho u_i) = 0 \tag{2}$$

Since density is assumed to be constant, then the equation becomes

$$\rho \frac{\partial u_i}{\partial x_i} = 0 \tag{3}$$

which in component form is given by

$$\frac{\partial u}{\partial x} + \frac{\partial v}{\partial y} + \frac{\partial w}{\partial z} = 0 \tag{4}$$

since the flow is in 2-dimensions in z and x direction, the equation becomes

$$\frac{\partial u}{\partial x} + \frac{\partial w}{\partial z} = 0 \tag{5}$$

3. Energy Equation

This is derived from Newton's second law of motion which states that the rate of change of momentum of a body is equal to the resultant force acting on the body. When a fluid is in motion there are forces that act on it which are in contact with the fluid and some act from a distance. Forces acting on a fluid particle from a distance are referred to as body forces while surface forces refer to the forces that are in direct contact with the fluid particles.

$$\rho c_p \frac{DT}{Dt} = K\nabla^2 T + \mu\Phi + \frac{J^2}{\sigma} \tag{6}$$

Where c_p is specific heat capacity at constant pressure, $\frac{DT}{Dt}$ is the material derivative, $\mu\Phi$ is the internal heating due to viscous dissipation and $(\frac{J^2}{\sigma})$ is the ohmic heating due to resistance of the electrolyte.
The final form of energy equation is as follows

$$\rho c_p\left[\frac{\partial T}{\partial t}+u\frac{\partial T}{\partial x}+w\frac{\partial T}{\partial z}\right]=K\left[\frac{\partial^2 T}{\partial x^2}+\frac{\partial^2 T}{\partial z^2}\right]+\mu\left[(\frac{\partial u}{\partial x})^2+(\frac{\partial w}{\partial z})^2\right]+\sigma u^2 B_0^2 \tag{7}$$

dividing all through by ρc_p

$$\left[\frac{\partial T}{\partial t}+u\frac{\partial T}{\partial x}+w\frac{\partial T}{\partial z}\right]=\frac{K}{\rho c_p}\left[\frac{\partial^2 T}{\partial x^2}+\frac{\partial^2 T}{\partial z^2}\right]+\frac{\mu}{\rho c_p}\left[(\frac{\partial u}{\partial x})^2+(\frac{\partial w}{\partial z})^2\right]+\frac{\sigma u^2 B_0^2}{\rho c_p} \tag{8}$$

4. Non-Dimensionalization

Non dimensionalization is a process that aims at ensuring that the results obtained from a study are applicable to other geometrically similar configurations under similar set of conditions. The method is of great generality and mathematical simplicity and starts with selecting a suitable scale against which all dimensions in a given physical model are scaled. The non dimensionalization of the governing equation is performed by selecting characteristic dimensionless quantities. Non-dimensionalization is used to discretize the governing equations by first selecting certain characteristics quantities and then substituting them in the equations.

The following non-dimensional quantities were used to non-dimensionalize the governing equations

$$u^*=\frac{u}{U_\infty},\quad w^*=\frac{w}{U_\infty},\quad w_0^*=\frac{w_0}{U_\infty},\quad t^*=\frac{U_\infty t}{h},\quad x^*=\frac{x}{h},\quad z^*=\frac{z}{h},\quad T^*=\frac{T-T_\infty}{T_w-T_\infty}$$

$$u=U_\infty u^*, w=U_\infty w^*, w_0=U_\infty w_0^*, t=\frac{h}{U_\infty}t^*, x=hx^*, z=hz^*, T=(T_w-T_\infty)T^*+T_\infty$$

The following partial derivatives in non-dimensional form will be substituted into the equations above:

4.1. Non-Dimensionalization of the initial and boundary conditions

At the entrance at $0\le z\le H$

$$t^*\le 0; u^*=0, v^*=0, w^*=0, T^*=0 \tag{9}$$

$$t^*>0, u^*=1, v^*=0, T^*=1 \tag{10}$$

At the exit:

$$t^*\ge 0, u^*=\frac{u}{U_\infty} and u=cx^2 \ and\ x=Hx^* \tag{11}$$

$$u^*=\frac{cx^2}{U_\infty}\ thus\ u^*=c\frac{(Hx^*)^2}{U_\infty}, v^*=0\ and\ w^*=w_0^* \tag{12}$$

$$T=T_w and T^*=\frac{T-T_\infty}{T_w-T_\infty}=\frac{T_w-T_\infty}{T_w-T_\infty}=1 \tag{13}$$

At the other surface:

$$t>0, u^*=0, v^*=0, T=T_\infty\ and\ T^*=\frac{T_\infty-T_\infty}{T_w-T_\infty}=0 \tag{14}$$

4.2. Non dimensionalization of the governing equations

Applying the non dimensionalization process the following equations were obtained.

$$\frac{\partial u^*}{\partial t^*}+u^*\frac{\partial u^*}{\partial x^*}+w_o^*\frac{\partial u^*}{\partial z^*}=\frac{1}{Re}(\frac{\partial^2 u^*}{\partial x^{*2}}+\frac{\partial^2 u^*}{\partial z^{*2}})-Mu^*-Xu^*+GrT^* \tag{15}$$

The above equation represent momentum equation in x-direction.

$$\frac{\partial w^*}{\partial t^*}+u^*\frac{\partial w^*}{\partial x^*}+w_o^*\frac{\partial w^*}{\partial z^*}=\frac{1}{Re}(\frac{\partial^2 w^*}{\partial x^{*2}}+\frac{\partial^2 w*}{\partial z^{*2}})-Xw^* \tag{16}$$

The above equation represent momentum equation in z-direction.

$$\frac{\partial T^*}{\partial t^*}+u^*\frac{\partial T^*}{\partial x^*}+w_o^*\frac{\partial T^*}{\partial z^*}=\frac{1}{Re}\frac{1}{Pr}(\frac{\partial^2 T^*}{\partial x^{*2}}+\frac{\partial^2 T^*}{\partial z^{*2}})+\frac{Ec}{Re}((\frac{\partial u^*}{\partial x^*})^2+(\frac{\partial w^*}{\partial x^*})^2)$$

$$+Re.R(u^*)^2 \tag{17}$$

The equation (28) represent the energy equation .

5. Method of Solution

The proposed method of solving the system of the non-linear equations that will be obtained for this particular flow problem is the numerical approximation method of finite differences. The method has inherent advantages such as it handles electrical problem more readily. The finite difference equations for $\frac{\partial U}{\partial t}$, $\frac{\partial U}{\partial x}$, $\frac{\partial U}{\partial y}$, $\frac{\partial^2 U}{\partial x^2}$, and $\frac{\partial^2 U}{\partial y^2}$ averaged at K and K+1 are used to give:

$$\begin{aligned}&\frac{U_{i,j}^{k+1}-U_{i,j}^{k}}{\Delta t}+U_{i,j}^{k+1}\left(\frac{U_{i+1,j}^{k+1}-U_{i-1,j}^{k+1}+U_{i+1,j}^{k}-U_{i-1,j}^{k}}{4(\Delta x)}\right)+w_0\left(\frac{U_{i,j+1}^{k+1}-U_{i,j-1}^{k+1}+U_{i,j+1}^{k}-U_{i,j-1}^{k}}{4(\Delta z)}\right)\\&=\frac{1}{Re}\left(\frac{U_{i+1,j}^{k+1}-2U_{i,j}^{k+1}+U_{i-1,j}^{k+1}+U_{i+1,j}^{k}-2U_{i,j}^{k}+U_{i-1,j}^{k}}{2(\Delta x)^2}\right)\\&+\frac{1}{Re}\left(\frac{U_{i,j+1}^{k+1}-2U_{i,j}^{k+1}+U_{i,j-1}^{k+1}+U_{i,j+1}^{k}-2U_{i,j}^{k}+U_{i,j-1}^{k}}{2(\Delta z)^2}\right)-XU_{i,j}^{k+1}-MU_{i,j}^{k+1}+GrT_{i,j}^{k+1}\end{aligned} \tag{18}$$

Making $U_{i,j}^{k+1}$ yields:

$$\begin{aligned}U_{i,j}^{k+1}=&\left[\frac{U_{i,j}^{k}}{\Delta t}-w_0\left(\frac{U_{i,j+1}^{k+1}-U_{i,j-1}^{k+1}+U_{i,j+1}^{k}-U_{i,j-1}^{k}}{4(\Delta z)}\right)+GrT_{i,j}^{k+1}+\right.\\&\left.\frac{1}{Re}\left(\frac{U_{i+1,j}^{k+1}+U_{i-1,j}^{k+1}+U_{i+1,j}^{k}-2U_{i,j}^{k}+U_{i-1,j}^{k}}{2(\Delta x)^2}+\frac{U_{i,j+1}^{k+1}+U_{i,j-1}^{k+1}+U_{i,j+1}^{k}-2U_{i,j}^{k}+U_{i,j-1}^{k}}{2(\Delta z)^2}\right)\right]\Bigg/\\&\left[\frac{1}{\Delta t}+\frac{U_{i+1,j}^{k+1}-U_{i-1,j}^{k+1}+U_{i+1,j}^{k}-U_{i-1,j}^{k}}{4(\Delta x)}+\frac{1}{Re(\Delta x)^2}++\frac{1}{Re(\Delta z)^2}+M+X\right]\end{aligned} \tag{19}$$

The finite difference equations for $\frac{\partial V}{\partial t}$, $\frac{\partial V}{\partial x}$, $\frac{\partial V}{\partial y}$, $\frac{\partial^2 W}{\partial x^2}$, and $\frac{\partial^2 W}{\partial y^2}$ averaged at k and k+1 are used to give:

$$\begin{aligned}&\frac{W_{i,j}^{k+1}-W_{i,j}^{k}}{\Delta t}+U_{i,j}^{k+1}\left(\frac{W_{i+1,j}^{k+1}-W_{i-1,j}^{k+1}+W_{i+1,j}^{k}-W_{i-1,j}^{k}}{4(\Delta x)}\right)+\\&w_0\left(\frac{W_{i,j+1}^{k+1}-W_{i,j-1}^{k+1}+W_{i,j+1}^{k}-W_{i,j-1}^{k}}{4(\Delta z)}\right)\\&=\frac{1}{Re}\left(\frac{W_{i+1,j}^{k+1}-2W_{i,j}^{k+1}+W_{i-1,j}^{k+1}+W_{i+1,j}^{k}-2W_{i,j}^{k}+W_{i-1,j}^{k}}{2(\Delta x)^2}\right)\\&+\frac{1}{Re}\left(\frac{W_{i,j+1}^{k+1}-2W_{i,j}^{k+1}+W_{i,j-1}^{k+1}+W_{i,j+1}^{k}-2W_{i,j}^{k}+W_{i,j-1}^{k}}{2(\Delta z)^2}\right)-XW_{i,j}^{k+1}\end{aligned} \tag{20}$$

Making $W_{i,j}^{k+1}$ yields:

$$W_{i,j}^{k+1} = \left[\frac{W_{i,j}^{k}}{\Delta t} - w_0 \left(\frac{W_{i,j+1}^{k+1} - W_{i,j-1}^{k+1} + W_{i,j+1}^{k} - W_{i,j-1}^{k}}{4(\Delta z)} \right) - U_{i,j}^{k+1} \left(\frac{W_{i+1,j}^{k+1} - W_{i-1,j}^{k+1} + W_{i+1,j}^{k} - W_{i-1,j}^{k}}{4(\Delta x)} \right) + \frac{1}{Re} \left(\frac{W_{i+1,j}^{k+1} + W_{i-1,j}^{k+1} + W_{i+1,j}^{k} - 2W_{i,j}^{k} + W_{i-1,j}^{k}}{2(\Delta x)^2} + \frac{W_{i,j+1}^{k+1} + W_{i,j-1}^{k+1} + W_{i,j+1}^{k} - 2W_{i,j}^{k} + W_{i,j-1}^{k}}{2(\Delta z)^2} \right) \right] \Big/ \left[\frac{1}{\Delta t} + \frac{1}{Re(\Delta x)^2} + \frac{1}{Re(\Delta z)^2} + X \right] \tag{21}$$

The finite difference equations for $\frac{\partial T}{\partial t}$, $\frac{\partial T}{\partial x}$, $\frac{\partial T}{\partial z}$, $\frac{\partial^2 T}{\partial x^2}$, and $\frac{\partial^2 T}{\partial z^2}$ averaged at k and k+1 used to give:

$$\begin{aligned} &\frac{T_{i,j}^{k+1} - T_{i,j}^{k}}{\Delta t} + U_{i,j}^{k+1} \left(\frac{T_{i+1,j}^{k+1} - T_{i-1,j}^{k+1} + T_{i+1,j}^{k} - T_{i-1,j}^{k}}{4(\Delta x)} \right) + \\ &W_{i,j}^{k+1} \left(\frac{T_{i,j+1}^{k+1} - T_{i,j-1}^{k+1} + T_{i,j+1}^{k} - T_{i,j-1}^{k}}{4(\Delta z)} \right) \\ &= \frac{1}{RePr} \left(\frac{T_{i+1,j}^{k+1} - 2T_{i,j}^{k+1} + T_{i-1,j}^{k+1} + T_{i+1,j}^{k} - 2T_{i,j}^{k} + T_{i-1,j}^{k}}{2(\Delta x)^2} \right) \\ &+ \frac{1}{RePr} \left(\frac{T_{i,j+1}^{k+1} - 2T_{i,j}^{k+1} + T_{i,j-1}^{k+1} + T_{i,j+1}^{k} - 2T_{i,j}^{k} + T_{i,j-1}^{k}}{2(\Delta z)^2} \right) + \\ &ReR\left(U_{i,j+1}^{k+1}\right)^2 + \frac{Ec}{Re} \left(\frac{U_{i+1,j}^{k+1} - U_{i-1,j}^{k+1} + U_{i+1,j}^{k} - U_{i-1,j}^{k}}{4(\Delta x)} \right)^2 + \\ &\frac{Ec}{Re} \left(\frac{W_{i,j+1}^{k+1} - W_{i,j-1}^{k+1} + W_{i,j+1}^{k} - W_{i,j-1}^{k}}{4(\Delta z)} \right)^2 \end{aligned} \tag{22}$$

Making $T_{i,j}^{k+1}$ yields:

$$T_{i,j}^{k+1} = \left[\frac{T_{i,j}^{k}}{\Delta t} - U_{i,j}^{k+1} \left(\frac{T_{i+1,j}^{k+1} - T_{i-1,j}^{k+1} + T_{i+1,j}^{k} - T_{i-1,j}^{k}}{4(\Delta x)} \right) - W_{i,j}^{k+1} \left(\frac{T_{i,j+1}^{k+1} - T_{i,j-1}^{k+1} + T_{i,j+1}^{k} - T_{i,j-1}^{k}}{4(\Delta z)} \right) + \frac{1}{RePr} \left(\frac{T_{i+1,j}^{k+1} + T_{i-1,j}^{k+1} + T_{i+1,j}^{k} - 2T_{i,j}^{k} + T_{i-1,j}^{k}}{2(\Delta x)^2} \right) + \frac{1}{RePr} \left(\frac{T_{i,j+1}^{k+1} + T_{i,j-1}^{k+1} + T_{i,j+1}^{k} - 2T_{i,j}^{k} + T_{i,j-1}^{k}}{2(\Delta z)^2} \right) + ReR\left(U_{i,j+1}^{k+1}\right)^2 + \frac{Ec}{Re} \left(\frac{U_{i+1,j}^{k+1} - U_{i-1,j}^{k+1} + U_{i+1,j}^{k} - U_{i-1,j}^{k}}{4(\Delta x)} \right)^2 + \frac{Ec}{Re} \left(\frac{W_{i,j+1}^{k+1} - W_{i,j-1}^{k+1} + W_{i,j+1}^{k} - W_{i,j-1}^{k}}{4(\Delta z)} \right)^2 \right] \Big/ \left[\frac{1}{\Delta t} + \frac{1}{RePr(\Delta x)^2} + \frac{1}{RePr(\Delta z)^2} \right] \tag{23}$$

6. Results and Discussions

6.1. Effects of varying Reynolds number on primary velocity

From Figure 2, it is observed that an increase in Reynolds number leads to an increase in the primary velocity profile. Reynolds number represents the ratio of the inertial forces to viscosity forces. Increase in Reynolds number results to a decrease in the viscous forces which is the force that is known to oppose the motion of the fluid. When Reynolds number (Re) is small, it means that the viscous forces are more dominant than the inertial forces and thus causes more drag in the fluid reducing the velocity of the flow. When Reynolds number (Re) is large, the inertia force is more dominant hence an increase in velocities.

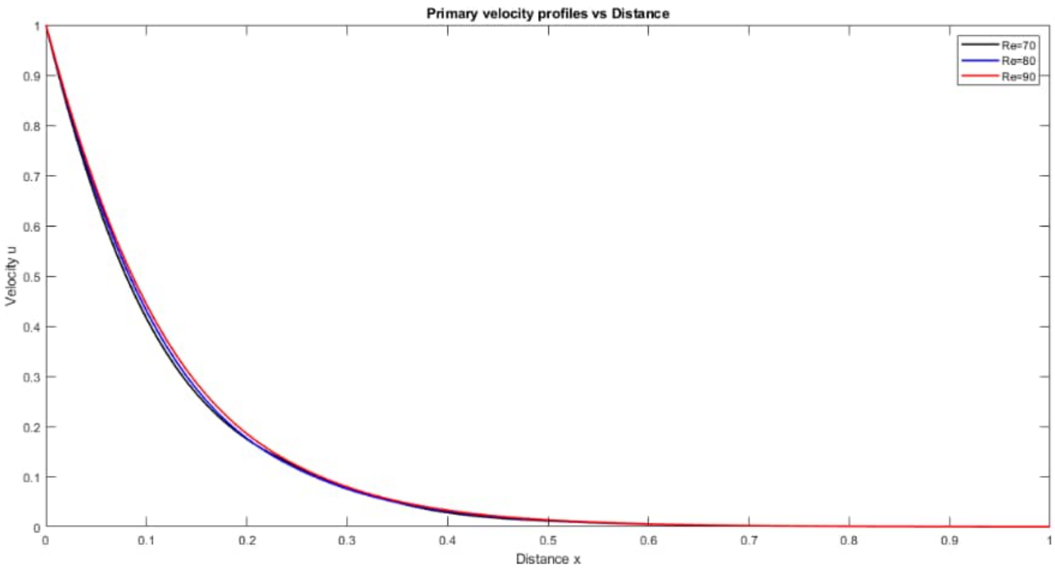

Fig. 2. Graph of dimensionless velocity profile for different values of the Reynolds number, Re

6.2. Effects of varying Magnetic number on primary velocity

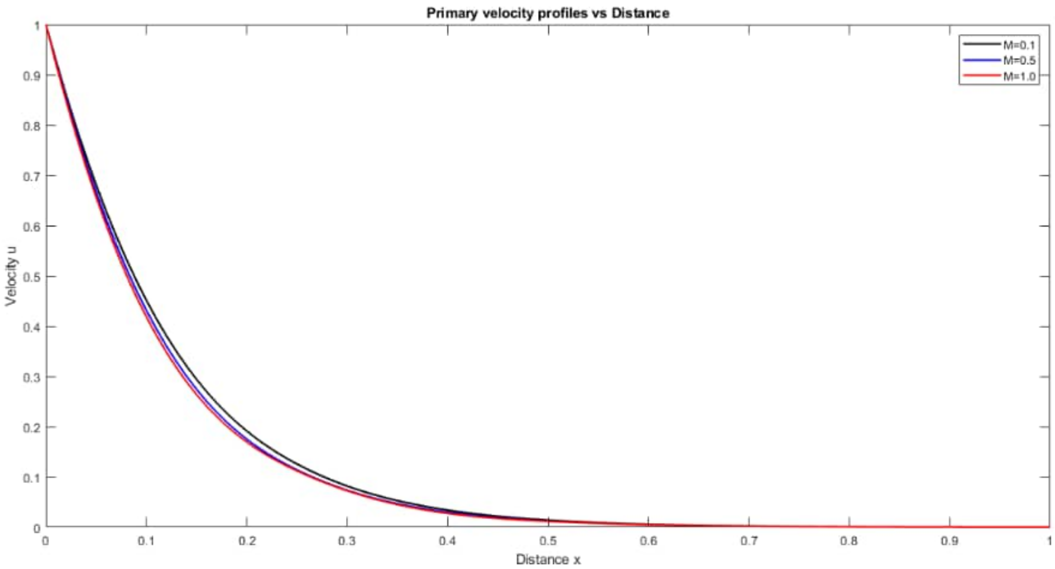

Fig. 3. Graph of dimensionless velocity profile for different values of the Magnetic number, M

From Figure 3, it is observed that an increase in magnetic parameter leads to a corresponding decrease in primary velocity of the flowing fluid. The presence of a transverse magnetic field in an electrically conducting flowing fluid creates Lorentz force which acts against the direction of the flow.

6.3. Effects of varying permeability parameter on primary velocity

From Figure 4 it is observed that an increase in permeability parameter (X) results to a decrease in primary velocity profile. The increase in permeability parameter leads to an increase in porosity of the medium which leads to a reduction in acceleration of the flow. Increased Permeability reduces the acceleration of the fluid flowing since the pores that would have allowed the fluid to flow with less restriction closes and as a result the primary velocity decreases.

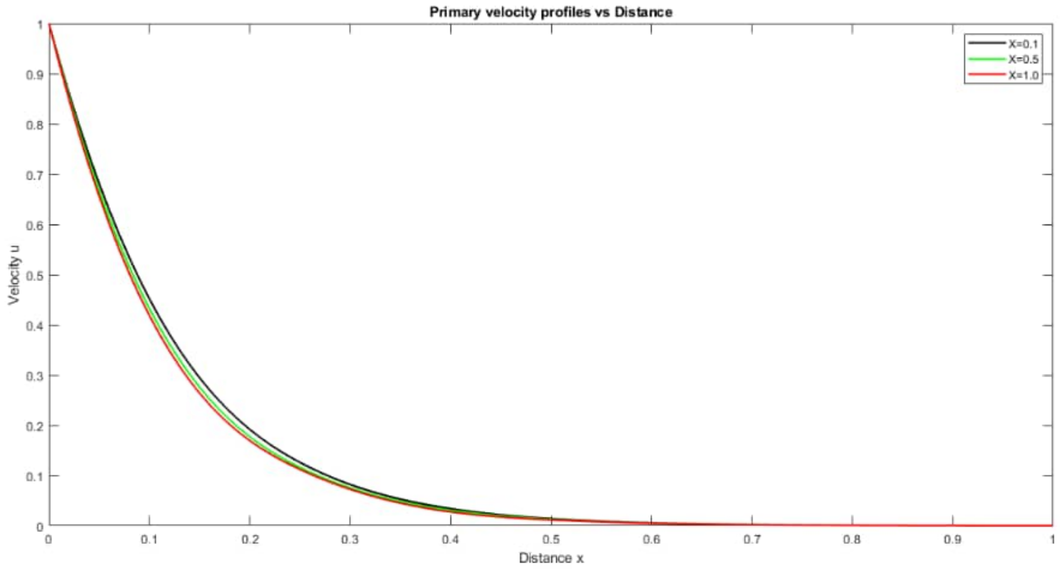

Fig. 4. Graph of dimensionless velocity profile for different values of the x number

6.4. Effects of varying Reynolds number on secondary velocity, Re

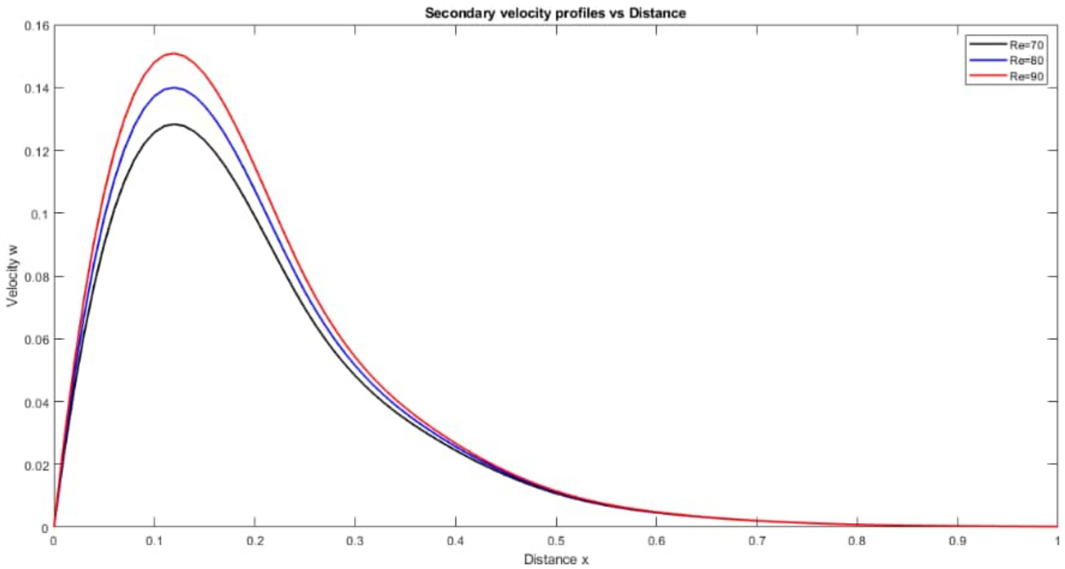

Fig. 5. Graph of dimensionless velocity profile for different values of the Reynolds number, Re

From Figure 5, it is observed that an increase in Reynolds number leads to an increase in the secondary velocity profile. Reynolds number represents the ratio of the inertial forces to viscosity forces. Increase in Reynolds number results to a decrease in the viscous forces which is the force that is known to oppose the motion of the fluid. When Reynolds number (Re) is small, it means that the viscous forces are more dominant than the inertial forces and thus causes more drag in the fluid reducing the velocity of the flow. When Reynolds number (Re) is large, the inertia force is more dominant hence an increase in velocities.

6.5. Effects of varying permeability parameter on secondary velocity

From Figure 6 it is observed that an increase in permeability parameter (X) results to a decrease in secondary velocity profile. The increase in permeability parameter leads to an increase in porosity of the medium which leads to a

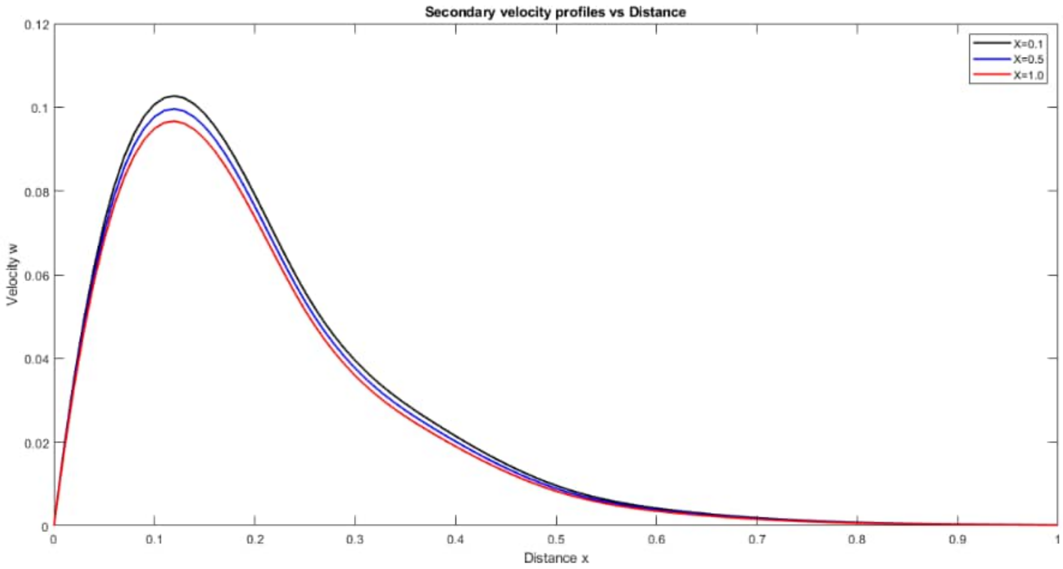

Fig. 6. Graph of dimensionless velocity profile for different values of the x number

reduction in acceleration of the flow. Hence reduction in secondary velocity profile.

6.6. Effects of varying Prandtl number on Temperature profile

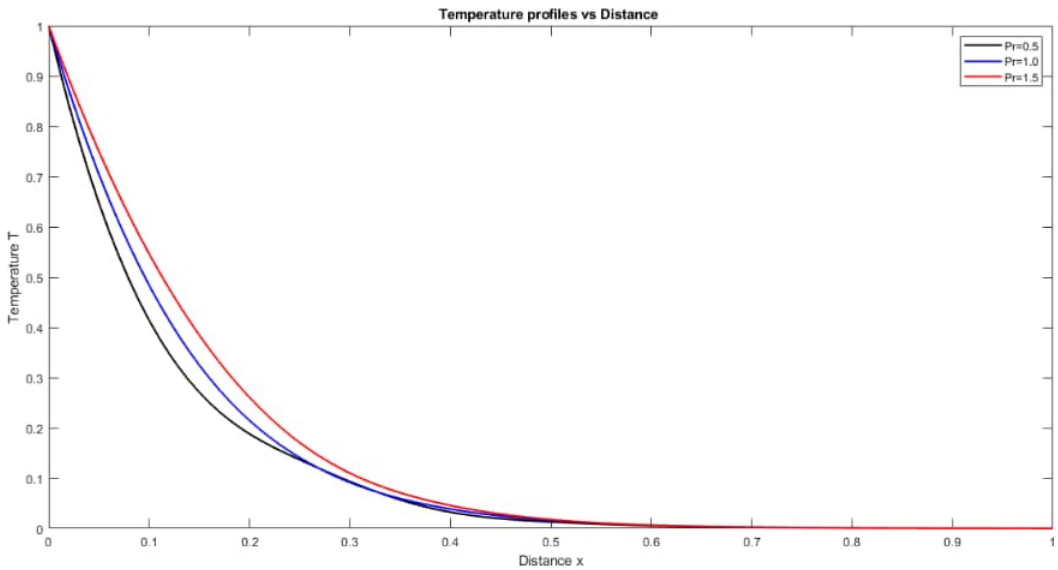

Fig. 7. Graph of dimensionless temperature profile for different values of the Pr number

From Figure 7, it is observed that an increase in Prandtl number leads to an increase in temperature profiles. Prandtl number is defined as the ratio of viscous diffusion rate to thermal diffusion. Increase in Pr means low thermal diffusivity of the fluid and as a result the fluid expands and the molecules moves apart hence leads to an increase in temperature.

6.7. Effects of varying Reynolds number on Temperature profile

From Figure 8, it is observed that an increase in Reynolds number leads to an increase in the temperature profile. Reynolds number represents the ratio of the inertial forces to viscosity forces. Increase in Reynolds number results

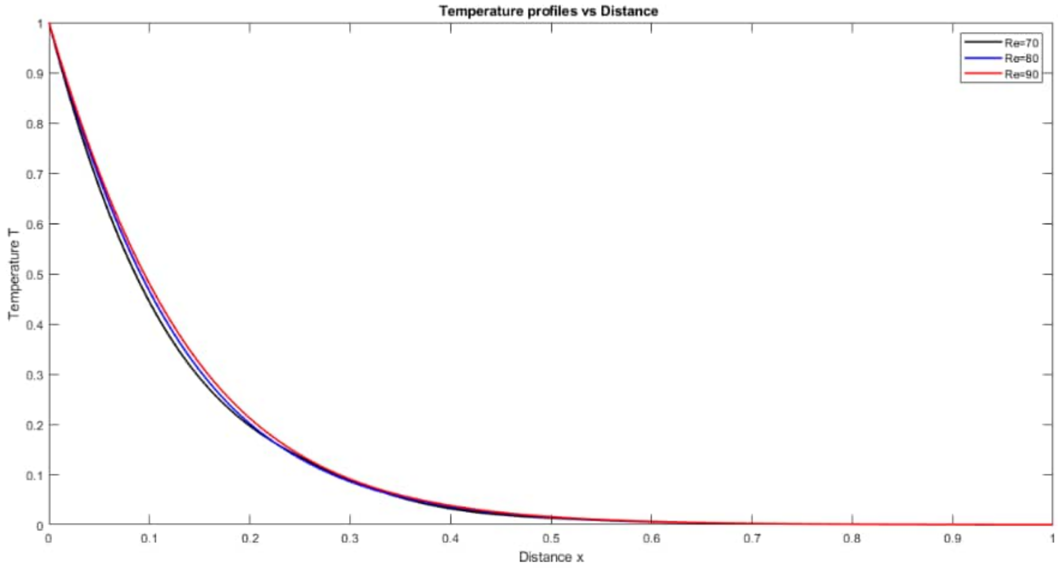

Fig. 8. Graph of dimensionless temperature profile for different values of the Re number

to a decrease in the viscous forces which is the force that is known to oppose the motion of the fluid. The increase in velocity creates an increase in collision of fluid particles, which leads to dissipation of heat in the boundary layer region, hence increase in temperature.

6.8. Effects of varying Eckert number on Temperature profile

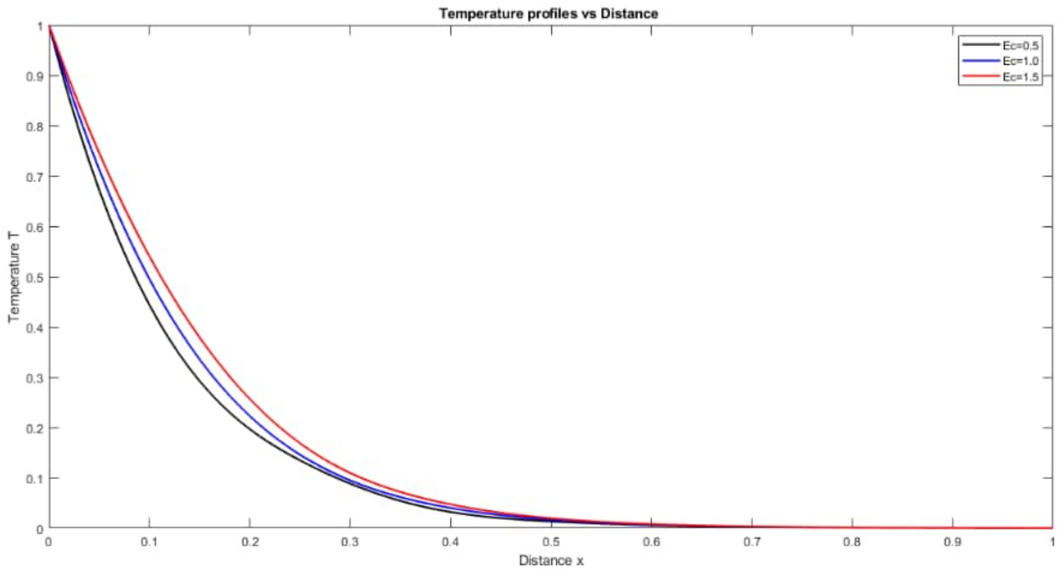

Fig. 9. Graph of dimensionless temperature profile for different values of the Ec number

From Figure 9, it is observed that an increase in the Eckert number (Ec) results to an increase in temperature of the fluid. An increase in Eckert number means that there is high kinetic energy which leads to increased collision of fluid particles. The increased collision results in dissipation of heat in the boundary layers hence an increase in temperature.

6.9. Effects of varying Joule heating parameter (R) Temperature profile

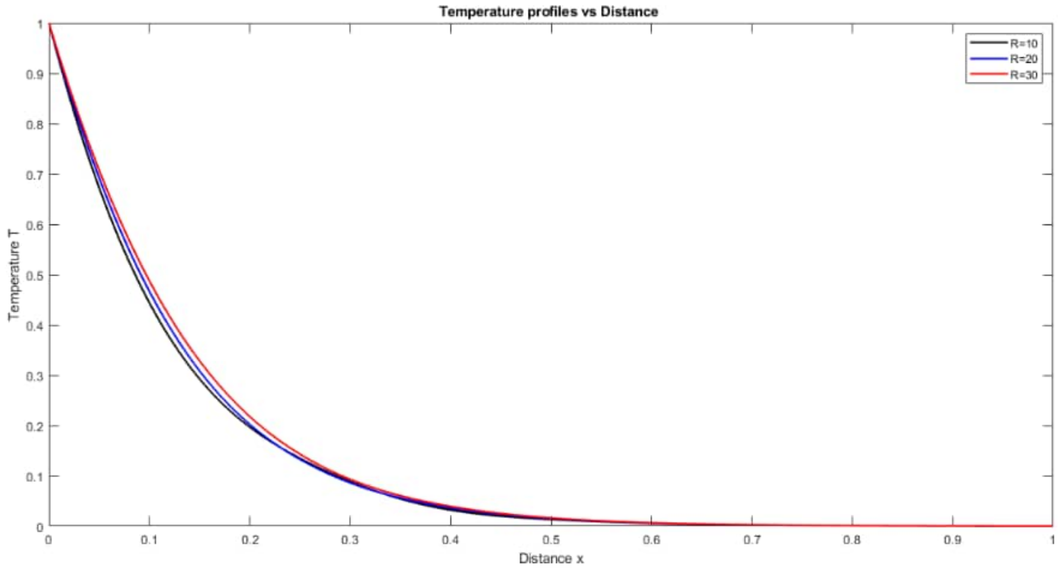

Fig. 10. Graph of dimensionless temperature profile for different values of the R number

From Figure 10, it is observed that an increase in joule heating parameter (R) leads to an increased in temperature. As the current is induced and starts flowing in the fluid, heat is generated due to the electrical resistance to the flow of charges and this leads to an increase in temperature.

7. Validation of Results

In the absence of Magnetic field, joule heating, suction and injection, the results agrees with [20] which had the following findings;

1. An increase in Reynolds number results to an increase in velocity and temperature profiles.
2. Increase in Eckert number leads to an increase in velocity and temperature profiles.
3. Increase in Prandtl number increases velocity profiles and temperature profiles.

8. Conclusions

It was noted that an increase in magnetic parameter leads to a decrease in both primary and secondary velocity profiles. Also an increase in suction/injection parameter leads to a decrease in both primary and secondary velocity profiles.
It was observed that an increase in Reynolds number leads to an increase in velocity and an increase in Magnetic and suction/injection parameter leads to a decrease in velocity. This implies that the fluid velocity is directly proportional to the Reynolds number and inversely proportional to magnetic and suction/injection parameter.
It was also observed that an increase in Prandtl number, Reynolds number, Eckert number and Joule heating parameter(R) leads to an increase in temperature of the fluid this is because temperature is directly proportional to the Prandtl number, Reynolds number, Eckert number and Joule heating parameter(R).

Acknowledgment

The authors would like to thank Jomo Kenyatta University support. Collins thanks Dr.Roy Kiogora of Jomo Kenyatta University of Agriculture and Technology and Prof. Kinyanjui of Jomo Kenyatta University of Agriculture and Technology, for their guidance throughout the development of this paper, especially for their insightful, constructive, and valuable comments.

References

[1] Boniface, K., Jackson, K., and Thomas, O. (2014). Investigation of hydro magnetic steady flow between two infinite parallel vertical porous plates. American Journal of Applied Mathematics, 2(5):170–178.

[2] Steenbrink, A. and Van der Giessen, E. (2016). On cavitation, post-cavitation and yield in amorphous polymer–rubber blends. Journal of the Mechanics and Physics of Solids, 47(4):843–876.

[3] Chandran, P., Sacheti, N. C., and Singh, A. (2015). Effect of rotation on unsteady hydromagnetic couette flow. Astrophysics and Space Science, 202(1):1–10.

[4] Nield, D., Kuznetsov, A., and Xiong, M. (2016). Thermally developing forced convection in a porous medium: parallel plate channel with walls at uniform temperature, with axial conduction and viscous dissipation effects. International Journal of Heat andMass Transfer, 46(4):643–651.

[5] Seth, G., Ansari, M. S., and Nandkeolyar, R. (2017). Effects of rotation and magnetic field on unsteady couette flow in a porous channel.

[6] Bodosa, G. and Borkakati, A. (2017). Mhd couette flow with heat transfer between two horizontal plates in the presence of a uniform transverse magnetic field. Theoretical and Applied Mechanics, 30(1):1–9.

[7] Makinde, O. and Mhone, P. (2019). Heat transfer to mhd oscillatory flow in a channel filled with porous medium. Romanian Journal of physics, 50(9/10):931

[8] Kinyanjui, M., Chaturvedi, N., and Uppal, S. (2013). Mhd stokes problem for a vertical infinite plate in a dissipative rotating fluid with hall current. Energy conversion and Management, 39(5-6):541–548.

[9] Rajput, U. and Sahu, P. (2016). Natural convection in unsteady hydromagnetic couette flow through a vertical channel in the presence of thermal radiation. Int. J. Appl. Math. Mech, 8(3):35–56.

[10] Johana, S. K., Okelo, J., Gatheri, F. K., Ngesa, J. O., et al. (2018). Magnetohydrodynamic (mhd) free convective flow past an infinite vertical porous plate with joule heating.

[11] Attia, H. A. (2018). Unsteady mhd couette flow of a viscoelastic fluid with heat transfer. Kragujevac J. Sci, 32:5–15.

[12] De Andrade, V. and Pereira, J. (2015). Gravitational lorentz force and the description of the gravitational interaction. Physical Review D, 56(8):4689.

[13] Mukhopadhyay, S. (2016). Analysis of boundary layer flow over a porous nonlinearly stretching sheet with partial slip at the boundary. Alexandria Engineering Journal, 52(4):563–569.

[14] Chandran, P., Sacheti, N. C., and Singh, A. (2017). Effect of rotation on unsteady hydromagnetic couette flow. Astrophysics and Space Science, 202(1):1–10.

[15] Kim, Y. J. (2018). Unsteady mhd convective heat transfer past a semi-infinite vertical porous moving plate with variable suction. International journal of engineering science, 38(8):833– 845.

[16] Job, V. M. andGunakala, S. R. (2016). Unsteadymhd free convection couette flowbetween two vertical permeable plates in the presence of thermal radiation using galerkin's finite element method. International Journal of Mechanical Engineering, 2(5):99–110. Johana, S. K., Okelo, J., Gatheri, F. K., Ngesa, J. O., et al. (2018).

[17] Jha, B. K., Samaila, A. K., andAjibade, A. O. (2015). Unsteady natural convection couette flow of a reactive viscous fluid in a vertical channel. Computational Mathematics and Modeling, 24(3):432–442.

[18] Joseph, K., Daniel, S., and Joseph, G. (2015). Unsteady mhd couette flow between two infinite parallel porous plates in an inclined magnetic field with heat transfer. International Journal of Mathematics and Statistics Invention, 2(3):103–110.

[19] Raptis, A. and Kafousias, N. (2016). Magnetohydrodynamic free convective flow and mass transfer through a porous medium bounded by an infinite vertical porous plate with constant heat flux. Canadian Journal of Physics, 60(12):1725–1729.

[20] Chauhan, D. S. and Agrawal, R. (2015). Effects of hall current on mhd flow in a rotating channel partially filled with a porous medium. Chemical Engineering Communications, 197(6):830–845.

[21] Freidoonimehr, N., Rashidi, M. M., and Mahmud, S. (2015). Unsteady mhd free convective flow past a permeable stretching vertical surface in a nano-fluid. International Journal of Thermal Sciences, 87:136–145.

[22] Raptis, A. and Kafousias, N. (2015). Magnetohydrodynamic free convective flow and mass transfer through a porous medium bounded by an infinite vertical porous plate with constant heat flux. Canadian Journal of Physics, 60(12):1725–1729.

[23] Jha, B. K., Samaila, A. K., andAjibade, A. O. (2015). Unsteady natural convection couette flow of a reactive viscous fluid in a vertical channel. Computational Mathematics and Modeling, 24(3):432–442.